

Influence of nano size on various properties of $\text{Sn}_{1-x}\text{Co}_x\text{O}_2$ nanocrystalline

Diluted Magnetic Semiconductors

K. Srinivas and P. Venugopal Reddy*

Department of Physics, Osmania University,
Hyderabad, A.P, India -500007, * pvreddy@osmania.ac.in

ABSTRACT

With a view to understand the influence of nano size on various structural, electronic and magnetic properties of nanostructured $\text{Sn}_{1-x}\text{Co}_x\text{O}_2$, systematic Investigations have been carried out. After synthesizing the samples by sol-gel route, structural characterization was undertaken by XRD, TEM, FT-IR and Raman techniques. The samples are having the tetragonal rutile structure with single phase without any detectable impurity. The average particle sizes obtained from TEM are in the range of 18-48 nm. The reduction of intensities of Raman peaks, shift in their positions, their shape and size distribution are found to be influenced predominantly by the nano size of the materials. The optical band gap of the materials clearly indicates a red shift with increasing particle sizes. From XPS data, it has been observed that the oxidation state of Co is +2 and changes from low spin state to high spin state as the nano size of the materials increase. Further, the phonon confinement effect and electronic structure have been analyzed. The Magnetization studies clearly indicated the presence of room temperature ferromagnetism in these samples. Further, the analysis of the saturation magnetization, Coercive field clearly indicated that they critically depend on nano size of the materials.

Keywords: tartarate gel, diluted magnetic semiconductors, nano particles, electronic structure, optical properties,

1 INTRODUCTION

Diluted magnetic semiconductors (DMS), such as transition metal ions (Co, Mn, Ni, Fe, Cr etc.) doped with wide band gap semiconductors such as TiO_2 , ZnO , SnO_2 and HfO_2 etc., have been attracting considerable attention in recent years due to their great potential for novel applications in high-density magnetic storage, spintronics devices, bio-medical, magneto fluid and magneto-optical applications etc.,. However, it is of particular importance to understand the role of dimensionality in shaping the spin-polarized electronic structure of nanocrystalline oxide based DMSs because quantum confinement may result in intriguing ferromagnetic properties as they will be potentially useful. Apart from this, the synthesis of stable nanocrystalline DMSs with controllable grain size and surface morphology are of great fundamental and technological interest and has attracted much experimental efforts. Very few reports [1-4] on nanocrystalline Co-doped

SnO_2 powders rather than thin films have been reported with the conflicting results regarding the existence of the room temperature ferromagnetism. In the present work, systematic investigations have been made to understand the nano size dependent structural, electronic and magnetic properties and the results of such a study are presented here

2 EXPERIMENTAL

Nanocrystalline Co doped SnO_2 ($\text{Sn}_{0.95}\text{Co}_{0.05}\text{O}_2$) samples were prepared by the tartaric acid assisted sol-gel method. In this method, starting precursors were converted to tartarates and P^{H} was adjusted to a value between 5 - 6 by adding ammonia and tartaric acid. Later, ethylene glycol was added as a promoter of tartaric polymerization and also prevents the formation of Cobalt segregations during gelation. The solution was concentrated by slow evaporation (~16 hours) at 65 °C. After slow heating between, 140-160 °C the gel formed as a fluffy porous precursor resin. The prepared precursor was calcined at 200 °C for about 8 hrs and finally the powders were sintered at four different temperatures between 300 – 600°C for about 4 hrs. For comparison purposes, the undoped SnO_2 sample was also prepared in similar experimental conditions.

To understand the structural and morphological properties XRD, TEM, FT-IR and Laser Raman studies were undertaken. The electronic properties were studied using the optical absorption and XPS techniques. Finally, the magnetization measurements were undertaken using a Vibrating Sample Magnetometer (Model: DMSADE-1660 MRS) at room temperature by applying 15 kOe magnetic field.

3 RESULTS AND DISCUSSION

3.1 Structural properties

The XRD patterns of $\text{Sn}_{1-x}\text{Co}_x\text{O}$ ($x=0.05,0$) powder samples sintered at different temperature were shown in figure 1. It can be seen from these patterns that all the samples are found to exhibit tetragonal rutile structure and are also comparable with JCPDS data [Card No: 41-1445]. The lattice parameters a and c were obtained from (110) and (101) peaks using Scherer's formula and are presented in Table-1. It is clear from the table that there is no systematic variation of lattice parameter.

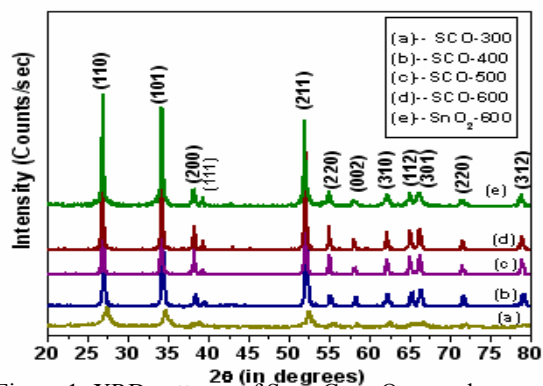


Figure 1: XRD patterns of $\text{Sn}_{0.95}\text{Co}_{0.05}\text{O}_2$ samples

Further, the average crystallite size of the samples (D) is determined from the diffraction peaks of (110) and (101), using peak broadening method and are in the range 15 nm-57 nm.

Table 1: XRD and TEM data for the $\text{Sn}_{1-x}\text{Co}_x\text{O}_2$ ($X = 0, 0.05$) samples.

Sample Name	Sintering Temp (°C)	<D> (nm)	Average Particle Size (nm)	<a> (°A)	<c> (°A)
SCO-300	300	15	18	4.741	3.155
SCO-400	400	24	25	4.726	3.177
SCO-500	500	32	35	4.711	3.163
SCO-600	600	40	45	4.719	3.173
SO-600	600	57	60	4.683	3.155

To investigate the chemical functional groups, FTIR spectra of all the samples were also recorded and are shown in Fig. 2. Several bands due to fundamentals, overtones and combinations of OH, Sn-O and Sn-O-Sn entities appear in $700-400\text{ cm}^{-1}$ range. The low wave number region exhibits a strong vibration around 618 cm^{-1} which corresponds to antisymmetric Sn-O-Sn mode of tin oxide. The widening of SnO₂ related bonds with increasing sintering temperature indicate, improvement in the crystallinity by strengthening O-Sn-O bonds with removal of organic impurities involved in the synthesis process.

Figure 3. represents the room temperature Raman spectra of all the samples. The peaks appeared around at 574 and 593 cm^{-1} undoped and Co doped samples are clear indication of nano crystalline behaviour. The most intense A_{1g} mode position is found to shift gradually from 616 to 631 cm^{-1} and the observed behavior clearly indicates the phonon confinement effect in the lattice. Raman bands around at 475 and 776 cm^{-1} are the vibrational modes E_g and B_{2g} , respectively. In fact, all these

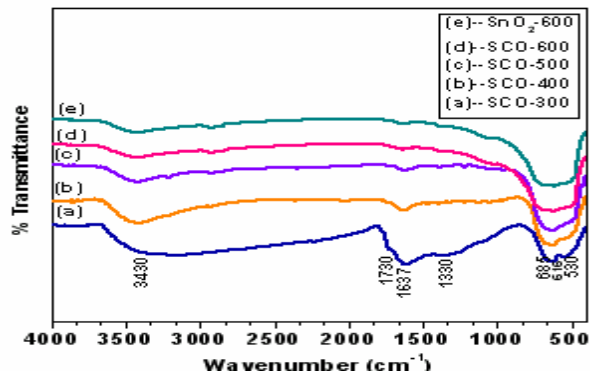


Figure 2: FTIR spectra of Co doped SnO_2 samples ($x = 0, 0.05$), sintered at different temperatures.

peaks are comparable with those reported in the literature [5-8]. Further, two new bands around at 306 and 695 cm^{-1} with less intensity, whose origin is controversial, were also observed. As a matter of fact, both these peaks were also observed in the case of undoped SnO_2 sample also. These peaks are neither due to parasitic phases nor due to the insertion of Co in the SnO_2 lattice in our case and may be originated from the defects such as oxygen vacancies. It is interesting to note from the Raman spectra that the peak intensities of doped samples are found to decrease continuously when compared with the undoped one. As the peak intensity is directly correlated with the insertion of Co in the SnO_2 matrix, the systematic changes in the peak positions and shapes clearly indicate the influence of nanosize on local structure and distribution of magnetic ions.

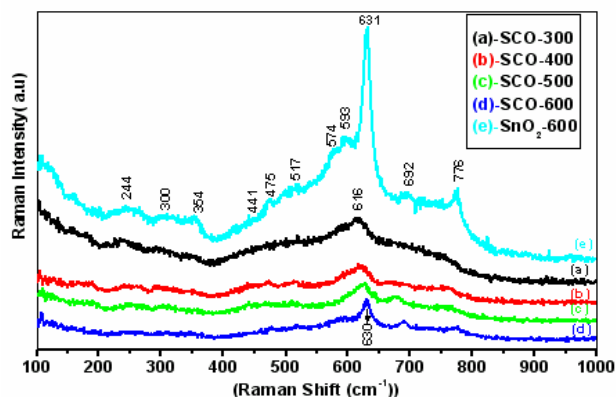


Figure 3: Raman spectra for nanocrystalline Co doped SnO_2 samples ($x = 0, 0.05$), sintered different temperatures.

Figure 4. illustrates the morphology and the electron diffraction patterns (shown inset) of the samples. It has been observed that the average particle sizes obtained from TEM are found to be in the range 18-48 nm [Table-1]. Incidentally, the crystallite size values obtained from Scherer's formula using XRD data are in agreement with those obtained from TEM studies. A close observation of TEM morphology images with increasing sintering temperature clearly indicate that the nano particles might

have aggregated and the observed behavior may be attributed to the redistribution of surface atoms due to change in particle's size, shape and surface defects .

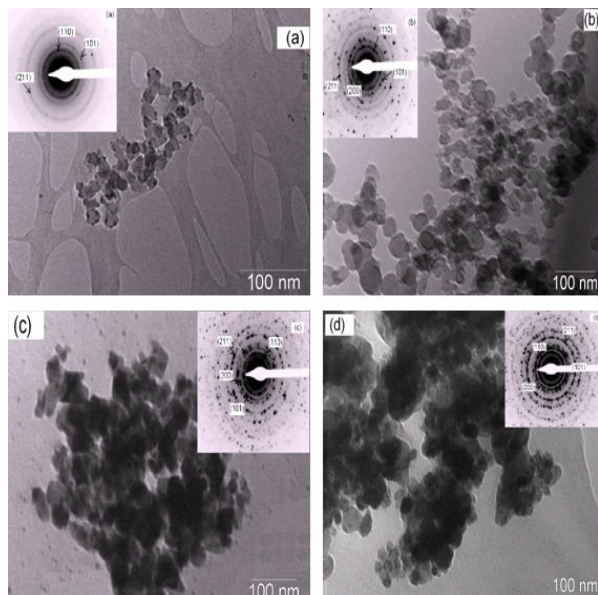


Figure 4: TEM morphology and SAD patterns (shown inset) for the Co doped SnO₂ samples.

3.2. Electronic properties

The electronic properties of all the samples were investigated using XPS and optical absorption measurements. The core level binding energy values of Co 2p_{3/2} and Co 2p_{1/2} peaks are shown in figure 5. and the values are given in Table-2. It can be seen that B.E values are found to shift towards higher side with decreasing particle size of the samples. One may therefore conclude that the nano size of the samples clearly influence the electronic structure and this may be attributed due to local structural changes associated with variation of particle size and non uniform strain. By comparing the binding energies of the cobalt core level XPS peaks with those in the literature and [9], it has been concluded that the oxidation state of Co in Sn_{0.95}Co_{0.05}O₂ samples is +2. Further, two shake-up satellite peaks, as specific evidence and it changing from low spin Co²⁺ state to high spin Co²⁺ with increasing sintering temperature. There is no possibility of forming Co Clusters since the B.E of Co metal cluster is at 778.3 eV and the energy difference between Co 2p_{3/2} and 2p_{1/2} core levels for metallic Co is 14.97 eV which are not observed in the present investigation.

The room temperature absorption spectra of Co doped SnO₂ samples, sintered at different temperatures along with undoped SnO₂ shown in figure 6. The energy band gap values were estimated using second derivative approach and are given in Table-2 along with the particle size values of all the samples. In the Co doped SnO₂ samples upon Co doping, red shift in band gap values was exhibited where

as with decreasing particle size blue shift in the band gap values was demonstrated.

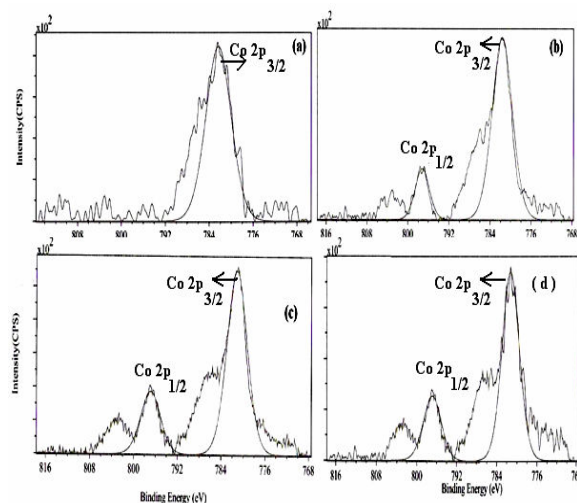


Figure 5: XPS core level deconvoluted spectra of Co 2p for the different particle sizes

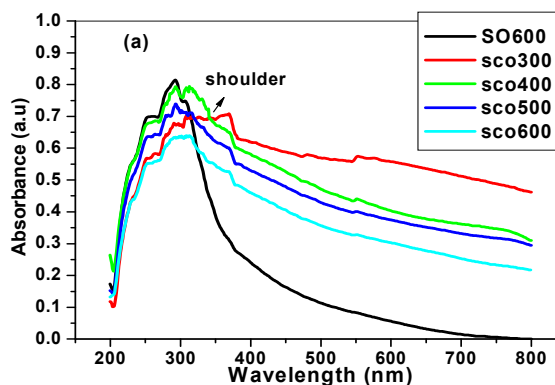


Figure 6: Optical absorbance DR spectra for Sn_{1-x}Co_xO₂ (X = 0.05, 0) powder samples

Table 2: Co XPS data Co element and optical band gaps for the Sn_{1-x}Co_xO₂ (X = 0.05, 0) powder samples with varying particle size.

Sample Code	Particle size (nm)	Binding Energy (e.V)		ΔB.E (eV)	E _g (eV)
		Co 2p _{3/2}	Co 2p _{1/2}		
SCO300	18	782.33	-	-	3.53
SCO400	25	781.66	797.25	15.99	3.47
SCO500	35	781.14	796.93	15.79	3.43
SCO600	45	780.47	794.76	15.39	3.32
SO-600	60	-	-	-	3.70

A shoulder is observed for photon energies right above the direct energy i.e.~3.6–3.9 eV and found to decrease its width with increasing sintering temperature. This appearance of shoulder is due to transitions, from the O(p)— states in the valence band to Sn(s)— states in the conduction band, occurring at points located near the Brillion Zone.

3.2. Magnetic properties

The magnetization measurements were performed using a vibrating sample magnetometer (VSM) at 300K and shown in figure 7. The obtained hysteresis curves exhibited that the $\text{Sn}_{1-x}\text{Co}_x\text{O}_2$ samples were all (except SCO300 sample) ferromagnetic at room temperature. The SCO300 sample might have impurities which are not removed completely as evidenced by FTIR and XPS. It is interesting to note that this is the first report which is reporting room temperature ferromagnetic samples of 5% Co doped SnO_2 nanocrystalline samples. The M_s and H_c values with varying particle size are given Table-3. The results revealed that the precise control of dopant distribution in the lattice and the particle size of the samples enormously influencing the local structure there by magnetic properties.

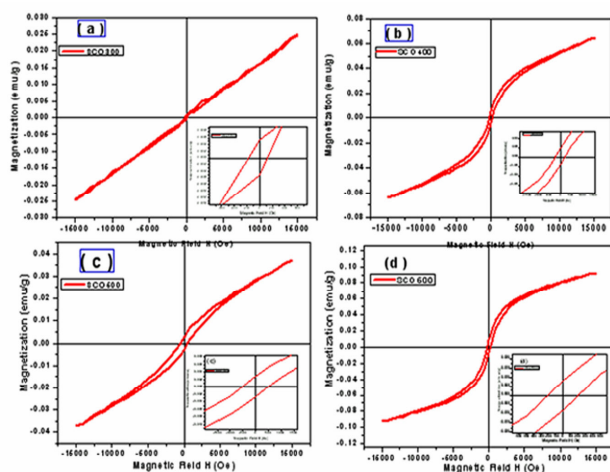


Figure 7: M-H Magnetization Curves for the $\text{Sn}_{0.95}\text{Co}_{0.05}\text{O}_2$ samples sintered at different temperatures.

In the present investigation the weak ferromagnetism obtained as a result of bound magnetic polarons (BMPs) coupled with adjacent randomly distributed Co^{2+} . The maximum obtained saturation magnetization value is 0.093 emu/g for the SCO600 sample. This rather small value can be explained by the fact that only a small portion of Co spins could be coupled ferromagnetically and the remaining Co are coupled either paramagnetic or antiferromagnetic when are coupled through oxygen vacancies with superexchange interaction.

The spontaneous magnetization (M_s) is decreases with D , suggesting the presence of a surface region (shell) with a reduced magnetization (M). The same behavior is reported earlier for soft magnetic nanoparticles [10]. The non-systematic changes indicating that the saturation magnetization of nano-particles depends not only on the magnitude of the individual atom or spin moment, but also on the particle size, shape or the complicated surface condition of the particles.

4 CONCLUSIONS

In summery, nanocrystalline $\text{Sn}_{0.95}\text{Co}_{0.05}\text{O}_2$ materials were synthesized with the average particle sizes in the

range of 18 – 45 nm by tartaric gel route without any additional impurity phases as evidenced by XRD, FTIR, Laser Raman and TEM studies. The gradual shift in A_{1g} mode position from 630 to 616 cm^{-1} with decreasing crystallite size, confirms the phonon confinement effect in the lattice.

The electronic studies using XPS and Optical absorbance measurements revealed that the nano size of the materials influences the binding energy values and optical band gap values predominantly.

Magnetic studies revealed that all the samples above sintered above 300 °C exhibited clear room temperature ferromagnetic behaviour. The values of saturation magnetization (M_s), and other related parameters depend on surface effects generated by changing the particle size and their distribution.

Table 3: Magnetization values for the $\text{Sn}_{1-x}\text{Co}_x\text{O}_2$ (X=0.05) samples sintered at different temperatures

Sample Code	M_s (emu/g)	H_c (Oe)	Average Particle size (nm)
SCO300	0.02456	150.091	18
SCO400	0.06430	215.170	25
SCO500	0.03714	478.047	35
SCO600	0.09292	209.232	45

REFERENCES

- [1] A. Bouaine and N. Brihi, G. Schmerber, C. Ulhaq Bouillet, S. Colis, and A. Dinia, J. Phys.Chem. C, 111, 2924,2007.
- [2] C.M. Liu, X.T.Zu and W.L. Zhou, J.Phys: Condens. Matter 18, 6001, 2006.
- [3] A. Punnose, M.H. Engelhard and J.Hays, Solid. State. Communi. 139, 434, 2006 and other Punnose et. al group references.
- [4] C.B. Fitzgerald, M.Venkatesan, A.P.Douvalis, S.Huber, J.M.D.Coey and T.Bakas, J.Appl.Phys.95, 7390, 2004.
- [5] S.H.Sun, G.W. Meng, G.X. Zhang, T.Gao, B.Y.Geng, L.D. Zhang and J.Zuo, Chem.Phys. letters 376, 103 2003.
- [6] Cunyi Xie, Lide Zhang, and Chimei Mo, Phys. Status Solidi A 141, K59 1994.
- [7] Soumen Das, Soumitra Kar and Subhadra Chaudhuri, J. Appl. Phys 99, 114303, 2006.
- [8] L. Abello, B. Bochu, A. Gaskov, S. Koudryavtseva, G. Lucazeau, and M. Roumyantseva, J. Solid State Chem. 135, 78, 1998.
- [9] J.F. Moulder, W.F. Stickle, P. E. Sobol, K. D.Bomben, "Handbook of X-ray Photoelectron Spectroscopy" (Perkin-Elmer Co., Eden Praine) 1992.
- [10]. R. Skomski, H. Zeng, M. Zheng, and D.J. Sellmyer, Phys. Rev. B 62, 3900, 2000.